Synthesis and Characterization of Hydrogel-Silver Nanoparticle-Curcumin Composites for Wound Dressing and Antibacterial Application

K. Varaprasad, Y. Murali Mohan,* K. Vimala, K. Mohana Raju

Department of Polymer Science and Technology, Synthetic Polymer Laboratory, Sri Krishnadevaraya University, Anantapur-515003, Andhra Pradesh, India

Received 27 July 2010; accepted 29 September 2010
DOI 10.1002/app.33508
Published online 24 February 2011 in Wiley Online Library (wileyonlinelibrary.com).

ABSTRACT: Hydrogel silver nanocomposites are found to be excellent materials for antibacterial applications. To enhance their applicability novel hydrogel-silver nanoparticle-curcumin composites have been developed. For developing, these composites, the hydrogel matrices are synthesized first by polymerizing acrylamide in the presence of poly(vinyl sulfonic acid sodium salt) and a trifunctional crosslinker (2,4,6-triallyloxy 1,3,5-triazine, TA) using redox initiating system (ammonium persulphate/TMEDA). Silver nanoparticles are generated throughout the hydrogel networks using *in situ* method by incorporating the silver ions and subsequent reduction with sodium borohydride. Curcumin loading into hydrogel-silver nanoparticles composite is achieved by diffusion mechanism. A series of hydrogel-silver nanoparticle-curcumin composites are developed and are characterized by using Fourier transform infrared (FTIR) and UV–visible (UV–vis) spectroscopy, X-ray diffraction, thermal analyses, as well as scanning and transmission electron microscopic (SEM/TEM) methods. An interesting arrangement of silver nanoparticles i.e., a shining sun shape (ball) ($\sim$ 5 nm) with apparent smaller grown nanoparticles ($\sim$ 1 nm) is observed by TEM. The curcumin loading and release characteristics are performed for various hydrogel composite systems. A comparative antimicrobial study is performed for hydrogel-silver nanocomposites and hydrogel-silver nanoparticle-curcumin composites. J Appl Polym Sci 121: 784–796, 2011

Key words: silver nanocomposites; poly(vinyl sulfonic acid sodium salt); hydrogels; curcumin; antibacterial activity; wound dressing

INTRODUCTION

Hydrogel nanocomposites are crosslinked hydrophilic polymers containing nanoparticles having capacity to absorb, swell and retain large amount of water in their crosslinked networks. In particular, the hydrogel nanocomposites in which the hydrogel matrix is combined with inorganic nanoparticles (NPs) have gained much attention during the past few years.[1] The size and shape of the inorganic nanoparticles can be controlled by the hydrogel internal network structures.[2] The hydrogel network structures are mainly regulated by the composition of various comonomers, polymers and crosslinkers that are employed in the synthesis of hydrogels.[3–5] The crosslinker plays a greater role in regulating the hydrogel networks structure which facilitate in tuning the size of the nanoparticles. A variety of crosslinkers namely *N,N′*-methylenebisacrylamide (MBA), *N,N′*-cystaminebisacrylamide (CBA), 1,4-butanediol diacrylate (BDDA) are used for this purpose.[6–11] On the other hand, freeze thaw technique can be used to create macro porous structures in hydrogels in which the nanoparticles can be developed.[12] In our recent investigation we have developed silver nanoparticles (Ag NPs) with different morphologies, i.e., nanorods, nanocubes and spherical nanoparticles by employing acrylic acid as comonomer in the hydrogel preparation.[13] The above hydrogel-nanoparticle composites are based on silver nanparticles due to their exponential use in the treatment of infections in burns, traumatic wounds, diabetic ulcers and antibacterial applications.[14–16] 1-10 nm silver nanoparticles are found as effective in the treatment of HIV-1.[17] The advantage of silver nanoparticles over silver ions is due to their "Enhanced Permeation and Retention" effects. Since, silver nanoparticles can enter inside the bacteria, fungus or virus and release the silver particles in a sustained manner thereby improving the overall therapeutic modalities.

**Present address:* Cancer Biology Research Center, Sanford Research/USD, Sioux Falls, SD-57105, USA.

Correspondence to: K. M. Raju (kmrmohan@yahoo.com).

Contract grant sponsors: Defense Research and Dev Organization, The Ministry of Defense, Govt. of India, New Delhi.

A number of antibacterial materials (Nanosilver: NanoCET, Mumbai, India, IonAumour: IONAURMOUR, Philadelphia, PA) and wound dressings (Acticoat-7: Smith and Newphew in UK; Actisorb Silver 220: Johnson and Johnson, New Brunswick, NJ; Aquacel-Ag hydrofiber: Convatec, Skillman, NJ) are commercially available. These nanosilver products are embedded in some polymer matrices or composite materials from which the release of AgNPs is not in a sustained manner. In view of this the present work involves the development of silver nanoparticles loaded in hydrogels. Curcumin (CUR) a hydrophobic polyphenolic compound derived from the rhizome of the herb *Curcuma longa*, possesses a wide range of biological activities including wound healing, antibacterial, antioxidant, anti-inflammatory and anticancer properties.[18]

To achieve novel and better antibacterial products, hydrogel-silver nanoparticle-curcumin composites are developed in the present investigation. For obtaining these products, poly(acrylamide)/poly(vinyl sulfonic acid sodium salt) (PAAm-PVSA) hydrogels are synthesized using a trifunctional crosslinker (2,4,6-triallyloxy-1,3,5-triazine, TA). The use of PVSA sodium salt in this study is due to its compatibility as well as possessing negatively charged sulfonate groups in their chains which are capable of attracting more number of silver ions and curcumin molecules.[19] Previous reports demonstrated that the incorporation of sulfonate groups into the substrate reduces protein adsorption or platelet adhesion.[20–22] In addition, PVSA sodium salt derived copolymeric hydrogels are good candidates for application as biomaterials in the areas of biosensors and actuators.[23] The trifunctional crosslinker can also influence the hydrogel networks and decides the nanoparticles structures. Incorporation of curcumin into these hydrogel nanocomposites will enhance further their antibacterial efficacy. Taking into consideration all the above factors the present work involves the development of poly(acrylamide)/poly(vinyl sulfonic acid sodium salt) silver nanoparticles (PAAm-PVSA-Ag NPs) hydrogels and poly(acrylamide)-poly(vinyl sulfonic acid sodium salt) silver nanoparticles-curcumin hydrogels composites for antibacterial and wound dressing applications.

MATERIALS AND METHODS

Materials

Acrylamide (AAm), poly(vinyl sulfonic acid, sodium salt) (PVSA) (25 wt % in water, technical grade), 2,4,6-triallyloxy 1,3,5-triazine (TA), ammonium persulfate (APS), *N,N,N′,N′′*-tetramethylethylenediamine (TMEDA), silver nitrate ($AgNO_3$), and sodium borohydride ($NaBH_4$) are purchased from Aldrich Chemicals Company (Milwakee, WI, USA). Curcumin (95% (w/w) Curcuminoids by Spectrophotometry) is a gift sample from M/s Natural Remedies Pvt. Ltd. (Bangalore, India). Double distilled water is used throughout the investigation for the preparation of solutions.

Preparation silver nanoparticles loaded hydrogels

The preparation of silver loaded hydrogels involves three steps as shown in Figure 1. These steps include[1] synthesis of hydrogel,[2] silver ions incorporation and[3] reduction of silver ions into silver nanoparticles.

Step 1

Hydrogels are prepared by solution polymerization in a 100 mL beaker following the procedure reported earlier with minor modifications.[9,10] The AAm (1 g, 14.08 m*M*) is dissolved in 4 mL of distilled water at ambient temperature (25°C). To this solution, 0.10 g of PVSA sodium salt and 1 mL of TA (1 g/100 mL, 4.01×10^{-3} m*M*) are added. Free radical crosslinking polymerization was carried out by adding 1 mL of ammonium persulphate (APS) (5 g/100 mL, 2.19×10^{-3} m*M*) and 1 mL of *N,N,N′,N′′*-tetramethylethylenediamine (TMEDA) (1 g/100 mL, 1.72×10^{-3} m*M*) as redox-initiating pair. A foam type bubble hydrogel was obtained within 30 min but to get complete networks throughout the hydrogels, the polymerization is continued for 8 h. The formed hydrogel samples are taken out from the beaker and washed them with distilled water and placed them in a 1-L beaker containing 500 mL distilled water (refilled fresh water for every 12 h for a week) to remove unreacted monomer/polymers from the hydrogels. Finally, the gels are dried at ambient temperature. Several samples are prepared by varying PVSA sodium salt and TA crosslinker concentrations (Table I).

Step 2

Dried hydrogels (500 mg) are allowed to swell in 100 mL distilled water at ambient temperature for 48 h and the swollen hydrogels are transferred to a beaker containing 50 mL of 0.1 m*M* silver nitrate aqueous solution for 24 h to reach equilibrium swelling. During this stage the silver ions are being exchanged from solution to the hydrogel network.

Step 3

The Ag+ ions loaded hydrogels are placed in 30 mL of 0.1 m*M* sodium borohydride aqueous solution and allowed for 2 h to reduce the silver ions into

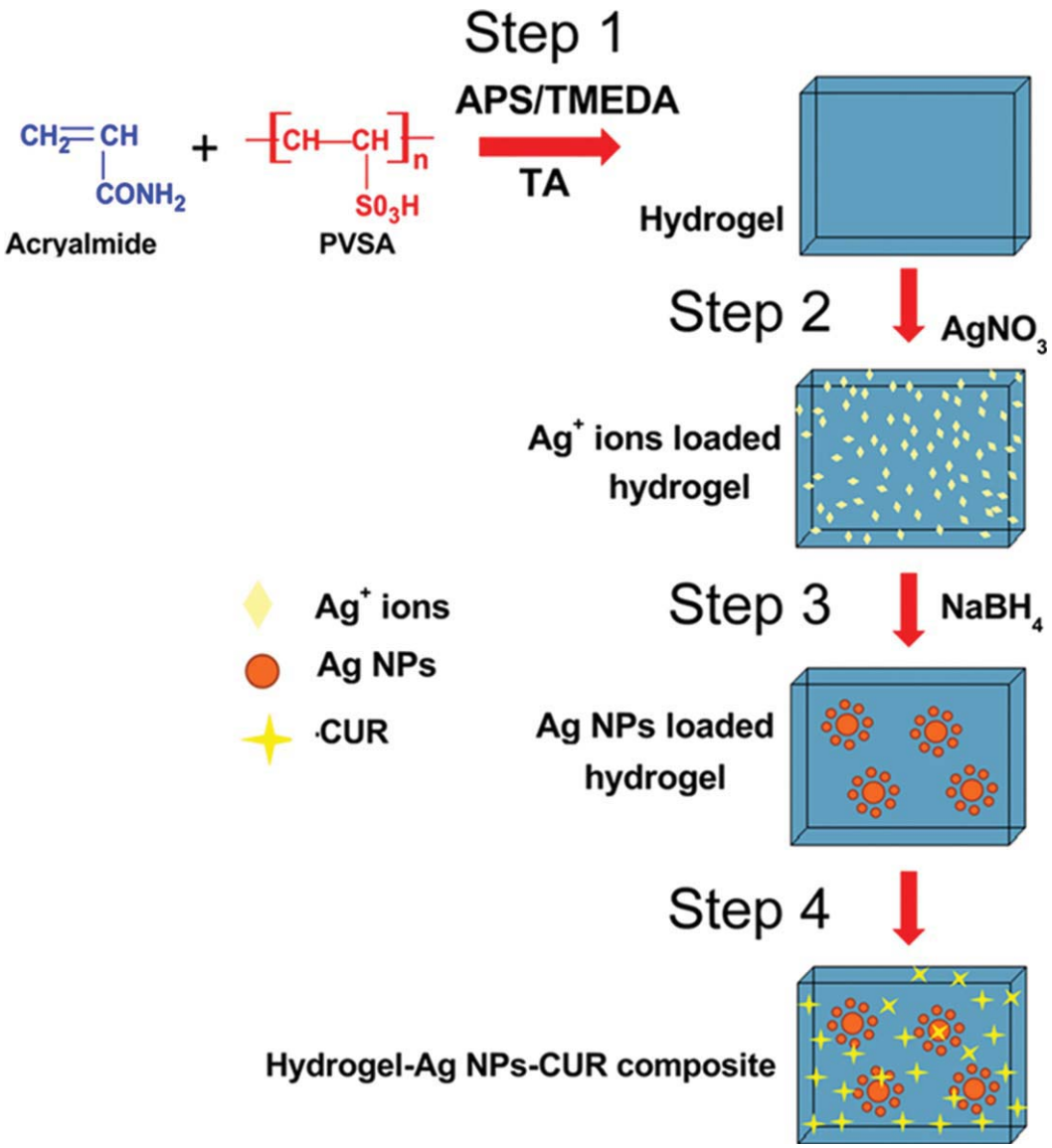

Figure 1 Synthetic route of for hydrogel-Ag NPs-curcumin composite. (Step 1) Polymerization of AAm and PVSA in the presence of crosslinker (TA) and initiating agents (APS/TMEDA). (Step 2) Incorporation of silver ions into hydrogel networks. (Step 3) Silver nanoparticles formation by sodium borohydride treatment. (Step 4) Curcumin loading into Ag NPs-hydrogel by diffusion mechanism. [Color figure can be viewed in the online issue, which is available at wileyonlinelibrary.com.]

silver nanoparticles with in the hydrogel network at 25°C. Finally, the obtained silver nanoparticles loaded hydrogels are dried at ambient temperature.

Curcumin loaded hydrogels

Curcumin (CUR) is loaded in Step 1, Step 2 and in Step 3 hydrogels by an absorption method (Step 4 in Fig. 1). Totally, 50 mg of hydrogels are allowed to swell in 20 mL of curcumin solution (5 mg/20 mL, 4:6 acetone:distilled water) for 24 h at 25°C in the dark (because curcumin is photosensitive). These gels are dried at 25°C in the dark. The loading efficiency of CUR in the hydrogels is monitored spectrophotometrically.[24] The drug-loaded hydrogels are placed in 50 mL of buffer solution (pH 7.4) and stirred vigorously for 160 h to extract the drug from the hydrogels. The solution is filtered and assayed by using UV spectrophotometer at a fixed λ_{max} value of 491.2 nm. The results of % drug loading and encapsulation efficiency are calculated using the following equations.

$$\% \text{ Drug loading} = [\text{weight of drug in the hydrogel} / \text{weight of hydrogel}] \times 100$$

$$\% \text{ Encapsulation efficiency} = [\% \text{ actual loading} / \% \text{ theoretical loading}] \times 100$$

TABLE I
Feed Composition of PAAm-PVSA Based Hydrogels

	Concentration in the feed mixture of gel networks				
Hydrogel code	AAm (m*M*)	PVSA (g)	TA (m*M*)×10^{-4}	APS (m*M*)×10^{-3}	TMEDA (m*M*)×10^{-3}
PVSA 1	14.08	0.10	4.01	2.191	1.721
PVSA 2	14.08	0.20	4.01	2..191	1.721
PVSA 3	14.08	0.30	4.01	2.191	1.721
PVSA 4	14.08	0.50	4.01	2.191	1.721
PVSA 5	14.08	0.10	2.00	2.191	1.721
PVSA 6	14.08	0.10	3.00	2.191	1.721
PVSA 7	14.08	0.10	5.01	2.191	1.721
PVSA 8	14.08	0.10	6.01	2.191	1.721

Swelling studies

The swelling characteristic of the hydrogels provides information of network integrity before and after loading of silver salt, precipitation of silver nanoparticles and curcumin encapsulation inside the networks. To evaluate the swelling behavior of hydrogels and hydrogel nanocomposites, ~ 20 mg weights of dried hydrogels are equilibrated in distilled water at 25°C for two days. After a given time interval, the gels are taken out from water, wiped off with filter papers and weighed using an electronic balance (AR0640 Ohaus Carp. Pine Brook, NJ). The swelling ratio (Q) of the gels is calculated from the equation: $Q = W_e/W_d$, where W_e is the weight of the swollen hydrogel at equilibrium and W_d is the dry weight of the pure hydrogel. The data provided is an average value of three samples reading.

Since the aim of this work is to employ these gels for antibacterial and wound dressing applications the swelling properties are also carried out in pseudo extracellular fluid **(**PECF**)** solution (simulated wound fluid), consisting of 0.68 g of NaCl, 0.22 g of KCl, 2.5 g of $NaHCO_3$ and 0.35 g of NaH_2PO_4 in 100 mL of distilled water.[25]

Characterization

Fourier transform infrared (FTIR) spectra are recorded on a Bruker IFS 66V infrared spectrophotometer (Ettlingen, Germany). The UV–vis spectra are recorded on an ELICO SL 164 Model UV–vis spectrophotometer (The Elico co, Hyderabad, India). The morphological variations are observed by using a JOEL JSM 840A (Tokyo, Japan) scanning electron microscope (SEM). For this study, samples are coated with a thin layer of palladium gold alloy just before image under SEM. Transmission electron microscopy (TEM) of the PVSA-silver nanocomposites are conducted on a Techai F12 (Tokyo, Japan) using an acceleration voltage of 15 kV. The TEM sample is prepared by dispersing two to three drops of (1 mg/1 mL) hydrogel-Ag NPs solution on 3 mm copper grid and dried at room temperature after removing excess solution using filter paper. X-ray diffraction analysis is carried out using a Model D/Max-2500Pc X-ray diffractometer (Rigagu, Tokyo, Japan) with CuKα radiation. Thermal analysis (DSC and TGA) of the samples were carried out using SDT Q 600 DSC instrument (T.A. Instruments-water LLC, Newcastle, DE 19720, USA) at a heating rate of 20°C/min under a constant nitrogen flow (100 mL/min).

Release of curcumin

To study the release pattern of curcumin from the loaded hydrogels, a known weight of curcumin loaded hydrogel is placed in 50 mL of 7.4 pH phosphate buffer at 37°C temperature. The released amount of curcumin is determined at different time intervals by recording the absorbance of the release medium by using UV–vis spectrophotometer ELICO SL 164 Model (The Elico Co, Hyderabad, India). The recorded absorbance is then related to the amount of curcumin released using a calibration plot (0.12–5% concentration). The absorption of the solutions of curcumin is measured at λ_{max} 491.2 nm.

Antibacterial activity

Method A

The antibacterial property of the developed samples is tested against *E-coli*. The agar medium is sterilized in a conical flask at a pressure of 15 lbs for 30 min. This agar is transferred into sterilized Petri dishes in a laminar air flan. After solidification of the media, *E-coli* culture is streaked on the solid surface of the media. To this inoculated Petri dish, one drop of gel solutions (20 mg/10 mL distilled water) are added using 10 μL tip and the plates are incubated for 48 h at 37°C.

Method B

To examine the antibacterial activity of the developed samples the bacterial growth (*E-coli*) is studied

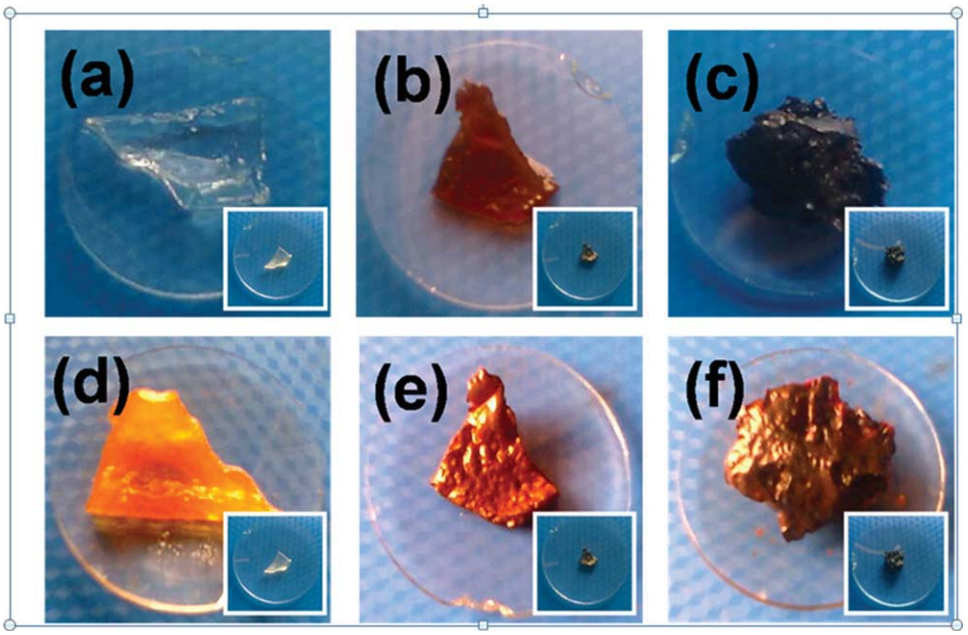

Figure 2 Dry and swollen hydrogel photographs. (A–C) Swollen hydrogel, Ag^+ ion loaded hydrogel, and Ag NPs loaded hydrogel (inset represent their respective dry gels, ~ 20 mg) and (D, E) Curcumin loaded into (A–C) hydrogels. All these hydrogel are based on PVSA5. [Color figure can be viewed in the online issue, which is available at wileyonlinelibrary.com.]

in mineral salt medium (MSM). This medium is prepared by with following composition in (g/L): NH_4NO_3 (1.5 g), KH_2PO_4 (2.5 g), K_2HPO_4 (0.5 g), NaCl (1.0 g), $MgSO_4$ (1.5 g), $MnSO_4$ (0.01 g), $FeSO_4$ (0.05 g), and $CaCl_2$ (0.05 g) are added into 1000 mL distilled water and the pH is adjusted to 7.0. Then the yeast extract (0.01%) is added for bacterial growth. After sterilizing the MSM, 50 mL of MSM solution is transferred into a sterilized 250 mL conical flask. Then 100 μL *E-coli* bacterium was added into the media. Finally, 100 μL of sample solution (20 mg/10 mL distilled water at 20°C) or its equivalent silver nanoparticles suspension is added and the optical density (OD) of the bacterial medium is measured using ELICO SL 164 Model UV–vis spectrophotometer (The Elico Co, Hyderabad, India) at 600 nm.

RESULTS AND DISCUSSION

The design of consumer products with antimicrobial properties is critically needed in the present living conditions. An ideal wound dressing or infection regulating products must have certain essential properties. They should perform basic functions such as provision and maintenance of moist environment, protection from secondary infections, absorption of wound fluids, macroporous environment for air exchange, painless with contact and must be easily removable.[26,27] For these applications, textile products embedded with silver salts or silver nanoparticles are being widely employed[28,29] but they are loosing their antibacterial properties after extensive washings. To overcome these limitations hydrogel films containing silver nanoparticles are developed.[9–11] The hydrogel-silver nanoparticle films exhibits good water absorption abilities and possess antimicrobial properties.

To improve further their applicability in wound/burn dressing the present work involves developing composite materials containing hydrogel (bio-compatibility), silver nanoparticles (antimicrobial), and curcumin (wound healing). This combinational approach will enhance their antibacterial efficacy and opens a new era in antimicrobial materials. For this purpose, P(AAm)/PVSA-Ag NPs hydrogel and P(AAm)/PVSA-Ag NPs-curcumin hydrogel composites are developed following the procedure illustrated in Figure 1.

Swelling properties

One important property of a wound dressing material is to have good hydration capacity which facilitates rapid wound healing and thereby improving the re-epithelialization process.[30] Therefore, evaluation of swelling capacity of hydrogels is an important requirement. The swelling behavior of hydrogels, hydrogel-Ag^+ ions, hydrogel-Ag NPs and their curcumin loaded hydrogels in water as well as in wound fluids (pseudo extracellular fluid, PECF) are studied. Figure 2 displays dry and swollen hydrogel as well as

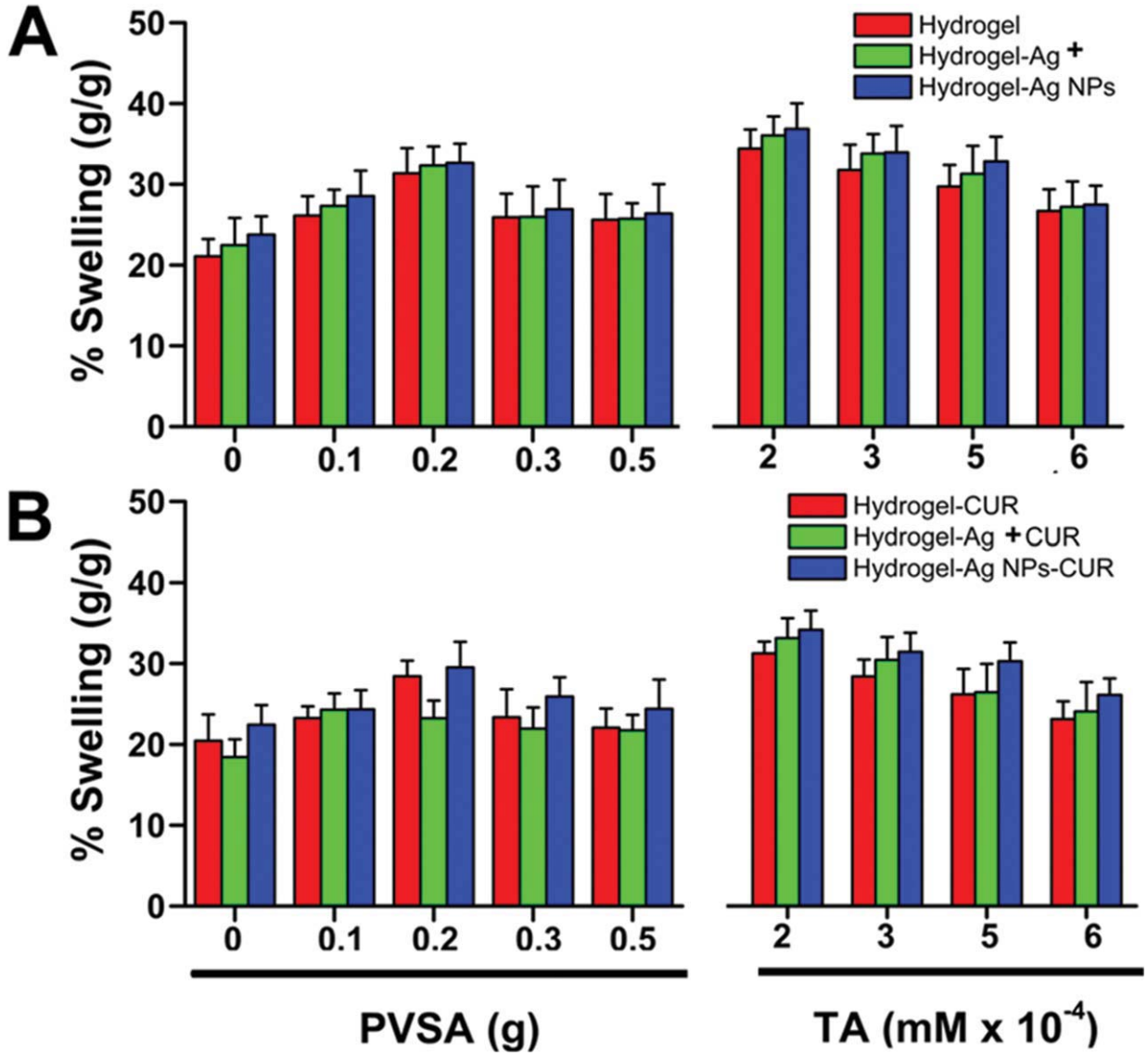

Figure 3 Swelling capacity of PAAm-PVSA hydrogels, hydrogels loaded with silver ions, silver nanoparticle formed hydrogels, in water. PVSA variation (PVSA1-4) hydrogel codes: AAm = 1 g (14.08 m*M*), PVSA = 0–0.5 g, TA = 4.01 × 10^{-4}, APS = 2.19 × 10^{-3}, TMEDA = 1.72 × 10^{-3}. Crosslinker (TA) variation (PVSA 5-8) hydrogel codes: AAm = 1 g (14.08 m*M*), PVSA = 0.1 g, TA = 2.00–6.01 × 10^{-4}, APS = 2.19 × 10^{-3}, TMEDA = 1.72 × 10^{-3}. [Color figure can be viewed in the online issue, which is available at wileyonlinelibrary.com.]

hydrogel composites. With increase of PVSA sodium salt concentration, the swelling capacity of the hydrogels in water increased initially and thereafter slightly decreased [Fig. 3(A)]. Where as, increase of TA concentration results in continuous drop in the swelling capacity of hydrogels in water [Fig. 3(A)]. The order of swelling capacity of hydrogels as observed is as follows; hydrogels loaded with Ag NPs > hydrogels loaded with Ag^+ ions > hydrogel. This behavior is attributed to the availability of more crosslinking sites for crosslink polymerization at higher PVSA concentration. Figure 3(A) also illustrates the effect of TA content on the swelling ratio of hydrogels (PVSA5-PVSA8) in swelling media. An increase of TA content (2.00 m*M* x 10^{-4} to 6.01 m*M* x 10^{-4}) in the hydrogel which result overall all hydrogels swelling property is decreases. Because of TA reduces the internal spaces in the hydrogel network. Whereas, increase of TA concentration results in continuous drop in the swelling capacity of hydrogels in water [Fig. 3(A)]. The order of swelling capacity of hydrogels as observed is as follows; hydrogels loaded with Ag NPs > hydrogels loaded with Ag^+ ions > hydrogel. Because of pure hydrogel were treated with $AgNO_3$ solution as a result of hydrogel have Ag+ ions which are making a more swelling ratio then pure hydrogels. Similarly Ag+ ions loaded hydrogels were treated with a $NaBH_4$ (reducing agent) solutions as a result of the Ag+ ions were converted into Ag nanoparticles with in the hydrogel network which are make a small pores

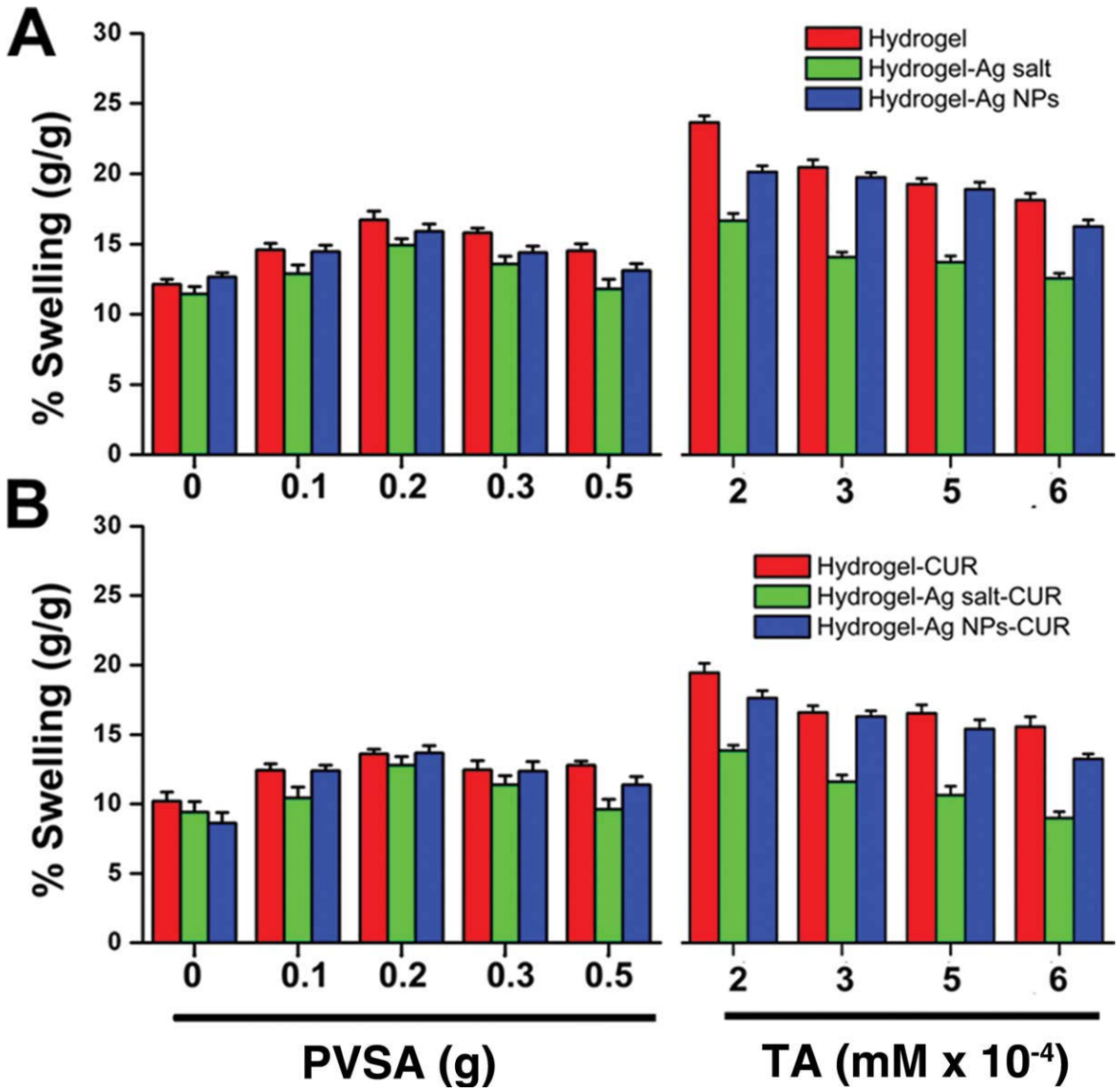

Figure 4 Swelling capacity of PAAm-PVSA hydrogels, hydrogels loaded with silver ions, silver nanoparticle formed hydrogels, in PECF solution. PVSA variation (PVSA1-4) hydrogel codes: AAm = 1 g (14.08 m*M*), PVSA = 0–0.5 g, TA = 4.01×10^{-4}, APS = 2.19×10^{-3}, TMEDA = 1.72×10^{-3}. Crosslinker (TA) variation (PVSA 5-8) hydrogel codes: AAm = 1 g (14.08 m*M*), PVSA = 0.1 g, TA = $2.00–6.01 \times 10^{-4}$, APS = 2.19×10^{-3}, TMEDA = 1.72×10^{-3}. [Color figure can be viewed in the online issue, which is available at wileyonlinelibrary.com.]

in said the hydrogels matrices as a resulting hydrogels uptake a more water. A similar pattern of swelling capacity is also observed for curcumin-loaded hydrogels except in some cases of PVSA sodium salt changed hydrogels [Fig. 3(B)]. A complete explanation of the swelling property of hydrogels can be found in our previous reports.[8–11,13,32]

The swelling capacity of these hydrogels is lower in PECF solution than in water (Fig. 4). In addition, the order of swelling capacity also differs i.e., hydrogel > hydrogels loaded with Ag NPs > hydrogels loaded with Ag^+ ions. This is due to the fact that the ionic strength of the medium influences the swelling capacity of ionic gels. All these observations indicate that the swelling capacities of the hydrogels synthesized in the present investigation are higher than those of PAAm hydrogels as well as many other natural and synthetic hydrogels.[9,10,29,31,32]

In situ silver nanoparticles formation

A distinct color change in solution is observed after *in situ* formation of silver nanoparticles in hydrogel as well as after the addition of Ag^+ ions into hydrogels (Fig. 1). To further confirm the *in situ* formation of silver nanoparticles, UV–vis spectra, X-ray diffraction, scanning electron microscopy (SEM), and transmission electron microscopic (TEM) studies are performed.

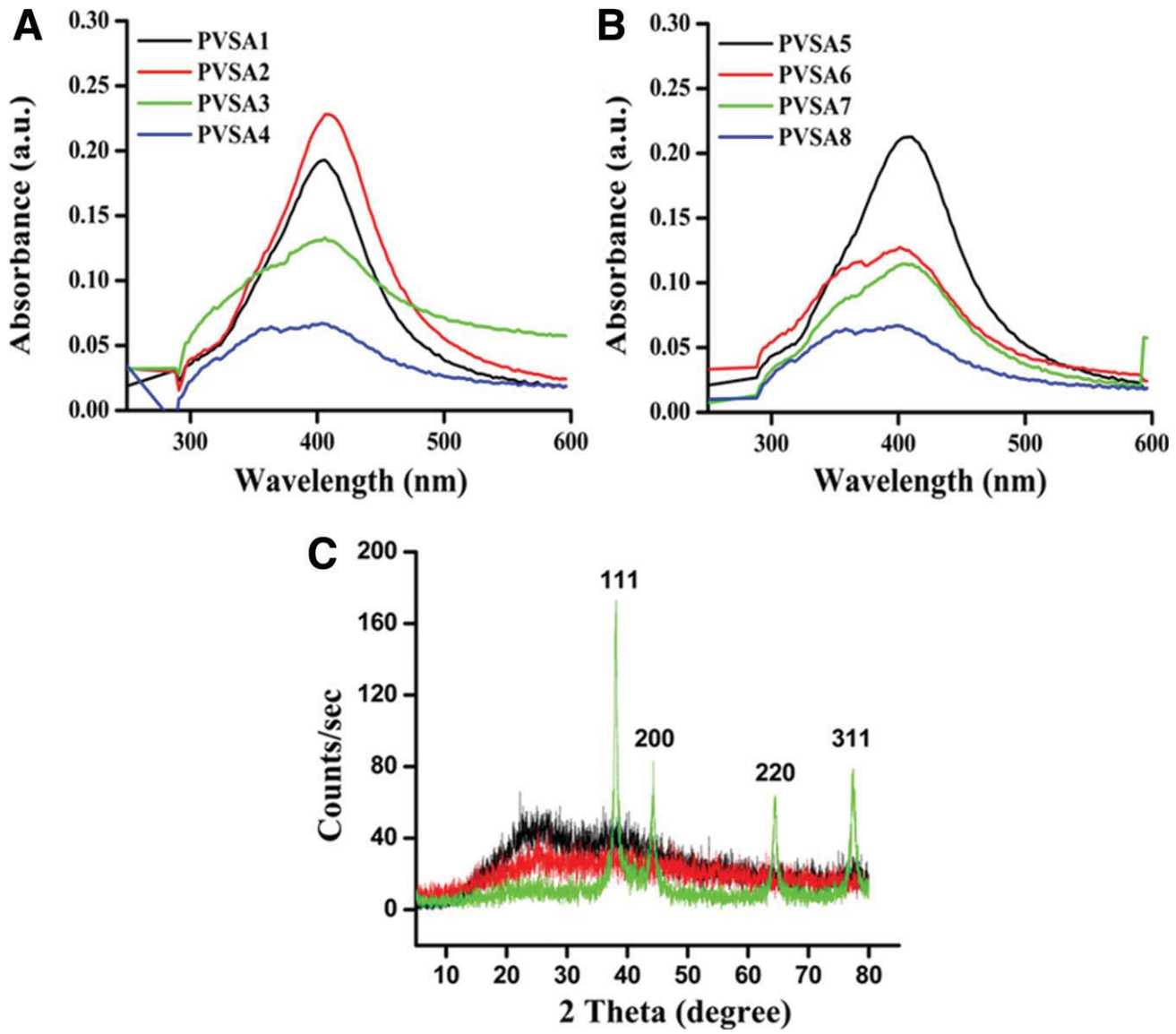

Figure 5 UV−vis spectral curves of hydrogel-Ag NPs solutions of (A) PVSA variation (PVSA1-4) hydrogel codes: AAm = 1 g (14.08 m*M*), PVSA = 0–0.5 g, TA = 4.01×10^{-4}, APS = 2.19×10^{-3}, TMEDA = 1.72×10^{-3}. (B) Crosslinker (TA) variation (PVSA 5-8) hydrogel codes: AAm = 1 g (14.08 m*M*), PVSA = 0.1 g, TA = 2.00–6.01×10^{-4}, APS = 2.19×10^{-3}, TMEDA = 1.72×10^{-3}. (C) X-ray diffraction of PVSA5, PVSA-Ag^{+} ions, and PVSA-Ag NPs hydrogels. [Color figure can be viewed in the online issue, which is available at wileyonlinelibrary.com.]

Silver nanoparticles loaded hydrogel solutions (1 mg/mL) have shown a distinct peak around 402–414 nm in the UV–vis spectra [Fig. 5(A,B)] due to Surface Plasmon Resonance effect caused by the quantum size of the silver nanoparticles.[33,34] The intensity of the absorbance band depends on the formulation. The absorbance intensity in the UV–vis spectra can be correlated with the swelling characteristic of hydrogels. The hydrogel having higher swelling capacity absorbs more number of silver ions and forms more silver nanoparticles in the networks which in turn shows higher intensity band in the UV–vis spectra. The formations of silver nanoparticles are clearly indicated by the absorption

TABLE II
UV−vis λ_{max} Absorbance Values of Solutions of PAAm-PVSA-Ag NPs Hydrogels

S. No.	SNCH code	λ max (nm)	Absorbency (%)
1	PVSA1	404.92	0.194
2	PVSA2	409.32	0.227
3	PVSA 3	404.92	0.132
4	PVSA 4	402.08	0.068
5	PVSA 5	414.22	0.213
6	PVSA 6	406.14	0.127
7	PVSA 7	407.43	0.114
8	PVSA 8	403.40	0.067

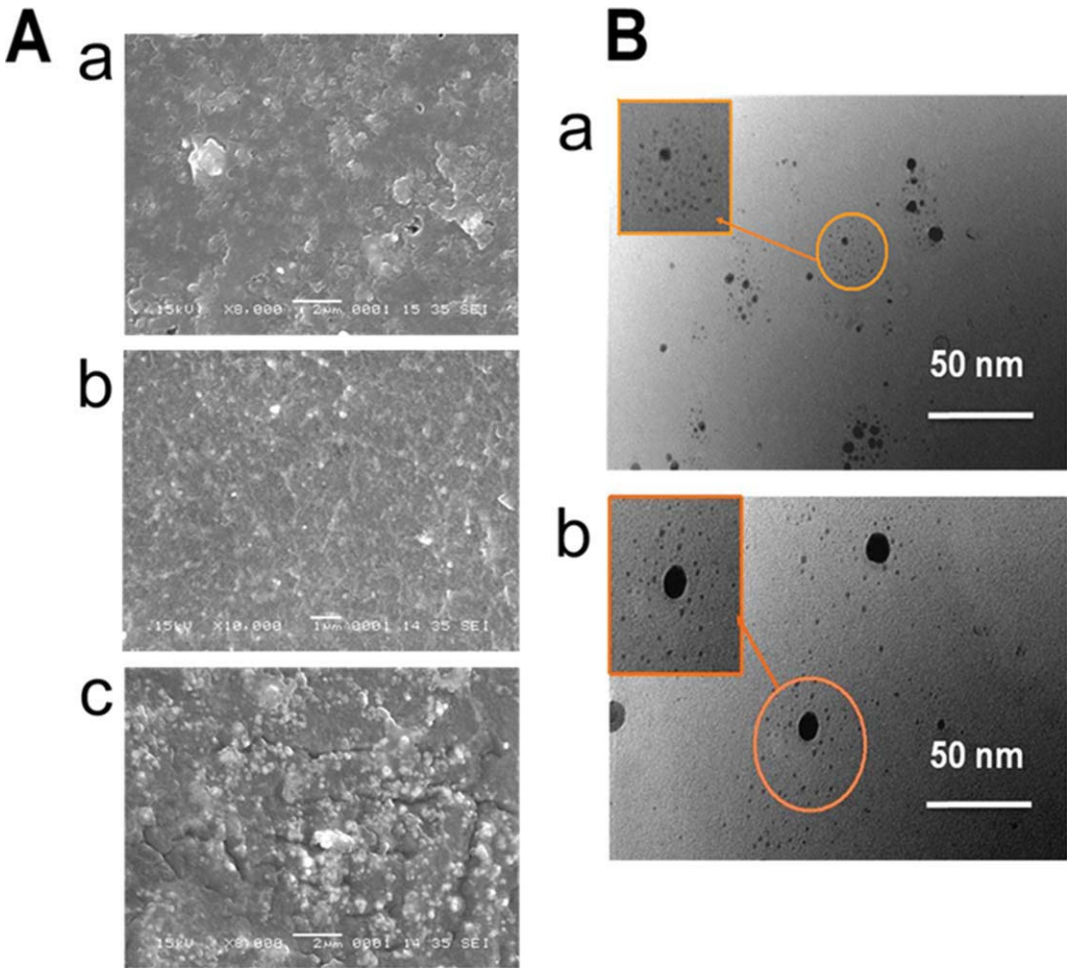

Figure 6 (A) SEM images of (a) PVSA5, (b) PVSA5-Ag^{+}, and (c) PVSA5-Ag NPs composite. (B) TEM images of silver nanoparticles extracted from (a) PVSA4-Ag NPs and (b) PVSA5-Ag NPs. [Color figure can be viewed in the online issue, which is available at wileyonlinelibrary.com.]

values of UV–vis spectra which are shown in Table II. The XRD pattern of hydrogel silver nanoparticles [Fig. 5(C)] has shown crystalline diffraction peaks at 2θ values of 38.09°, 44.27°, 63.93°, and 79.18° corresponding to, 111, 200, 220, and 311 intensities of the cubic silver phase(In the Joint Committee for Power Diffraction Studies database (PDF 4-783)).[20–22] Where as pure hydrogel and silver ions loaded hydrogel have not shown such type of peaks.

Scanning electron microscopic cross section analysis of hydrogel and silver ions loaded hydrogel has indicated rough morphologies where as silver nanoparticles loaded hydrogel has exhibited smaller nanoparticles throughout the gel networks [Fig. 6(A)]. A similar pattern of silver nanoparticles formation in hydrogel networks was observed in SEM studies.[9–11] The TEM images have clearly revealed the formation of smaller silver nanoparticles throughout the hydrogels network. The interesting aspect in the formation of silver nanoparticles, a spherical nanoparticle is being surrounded by few smaller nanoparticles [Fig.

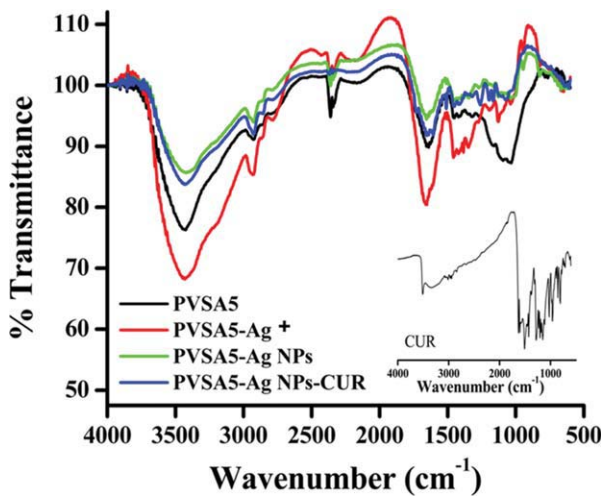

Figure 7 FTIR spectra of PVSA5, PVSA5-Ag^{+}, PVSA5-Ag NPs, and PVSA5-Ag NPs-curcumin composites. Inset represent FTIR spectrum of curcumin. [Color figure can be viewed in the online issue, which is available at wileyonlinelibrary.com.]

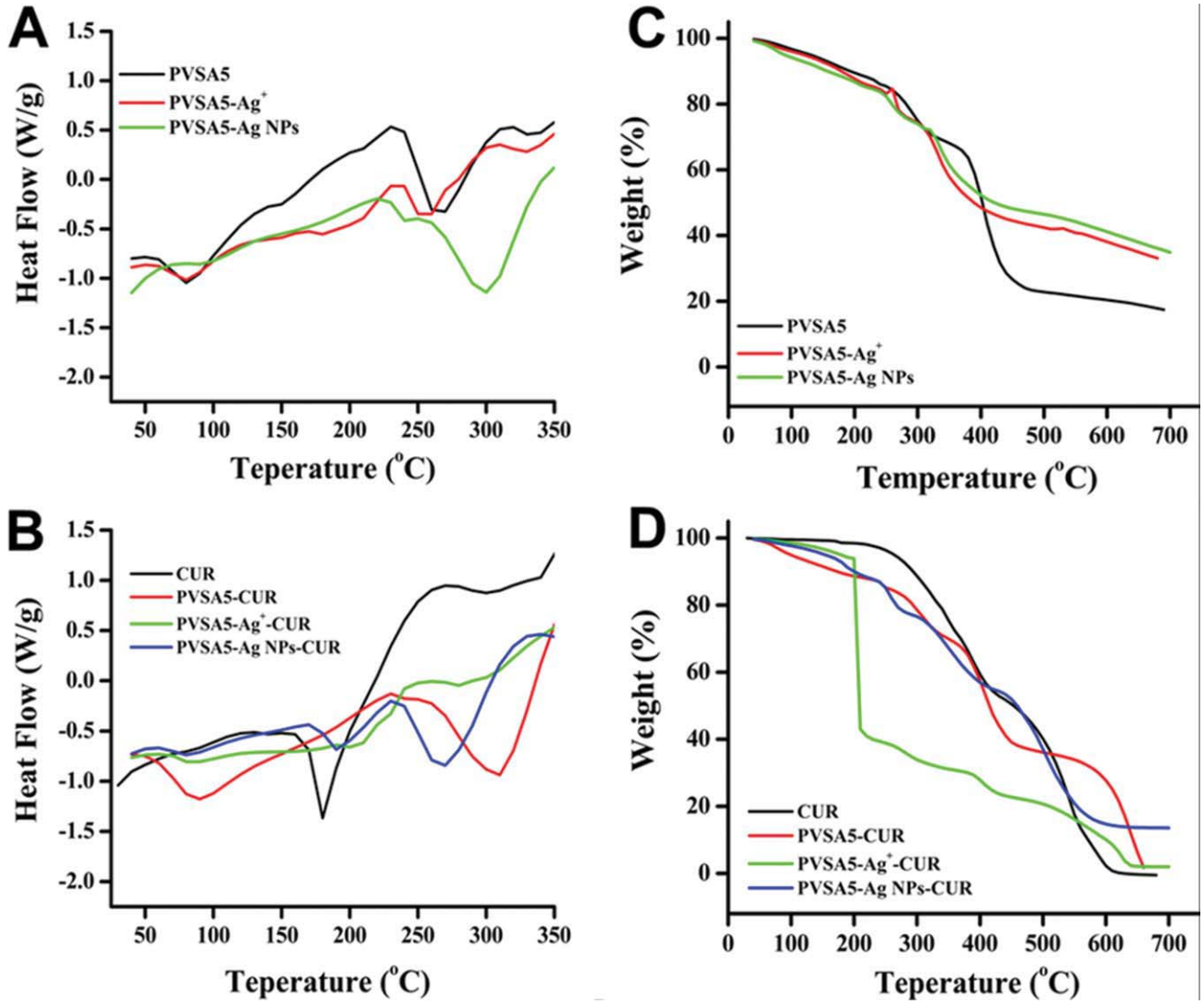

Figure 8 DSC and TGA curves of PVSA5, PVSA5-Ag^+ ion, PVSA5-Ag NPs-curcumin composites and their curcumin composites. [Color figure can be viewed in the online issue, which is available at wileyonlinelibrary.com.]

6(B)]. The magnification image has demonstrated beautiful formation like a shining sun (ball) shape of *ca.* ~ 5 nm with apparent smaller grown nanoparticles of *ca.* ~ 1 nm. This is achieved by changing either the polymer concentration or the trifunctional crosslinker concentration. Our earlier and other reports[9–11] have

TABLE III
% Encapsulation Efficiency and % of Cumulative Releases of Poly(AAm-PVSA) Hydrogels Data at pH 7 as well as Release Kinetics Parameters of Formulations at 37°C

Hydrogel code	% of encapsulation efficiency	n	k (10^2)	R^2	% of cumulative releases at various temperatures at their end time
PAAm-PVSA hydrogels					
PVSA2	43.4	0.70	0.53	0.99	93.93
PVSA 4	77.2	0.78	0.32	0.98	86.20
PVSA 5	65.5	0.44	1.00	0.95	96.58
Silver ions loaded PAAm-PVSA hydrogels					
PVSA2 + Ag^+	53.4	0.47	0.86	0.87	92.77
PVSA 4 +Ag^+	54.2	0.52	0.72	0.87	83.87
PVSA 5 +Ag^+	21.6	0.41	1.11	0.97	95.32
Silver nanoparticles loaded PAAm-PVSA hydrogels					
PVSA2 + Ag	87.9	0.96	0.04	0.99	97.30
PVSA 4 + Ag	88.4	1.11	0.42	0.99	87.72
PVSA 5 + Ag	79.2	0.89	0.12	0.97	99.66

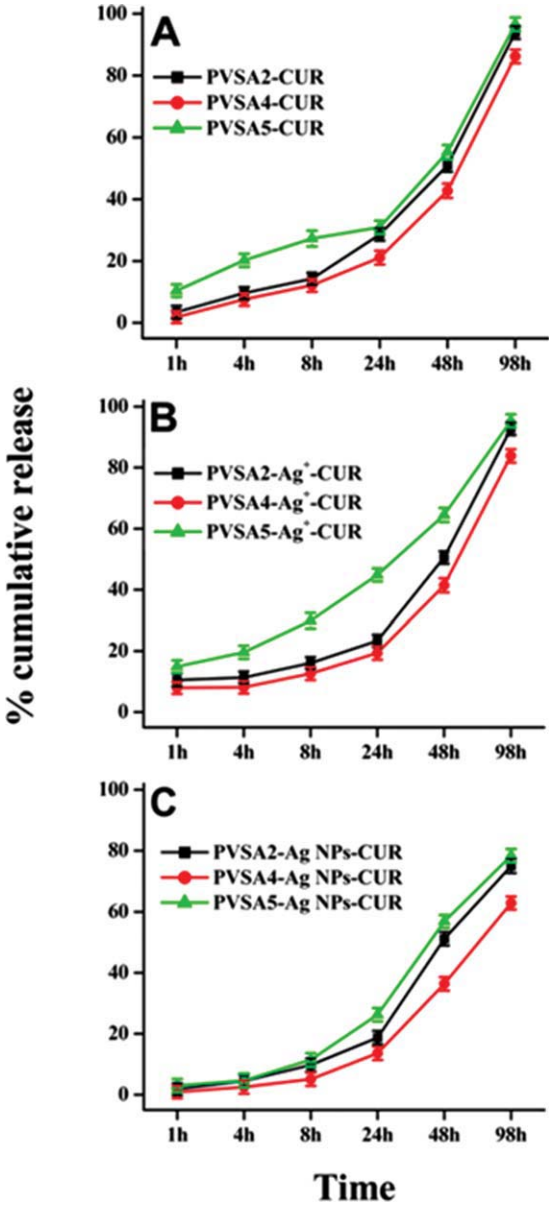

Figure 9 Cumulative release of curcumin PVSA2, PVSA4 and PVSA5, their silver ions loaded, and silver nanoparticles formed hydrogel composites. [Color figure can be viewed in the online issue, which is available at wileyonlinelibrary.com.]

demonstrated the formation of nanoparticles of size ranging from 3 to 10 nm but this is the first time to obtain this rare kind of morphology.

FTIR of hydrogel-Ag NPs-curcumin composite

To evaluate the presence of curcumin in the loaded hydrogel networks to have an effective function in antibacterial application, FTIR spectral analysis is performed (Fig. 7). FTIR spectrum of PVSA hydrogel has shown characteristic peaks of both PAAm and PVSA between 3300 and 3500 cm^{-1} (stretching vibrations of —OH/NH_2 of PAAm and/or hydrogen bonded peaks of PVSA), 2850–2950 cm^{-1} (symmetric and asymmetric stretching peaks of —CH_2 of PAAm/PVSA), 1680–1630 cm^{-1} (stretching vibration of —C=O of PAAm) and 1119.4–1040 cm^{-1} (absorption of peak of -SO_3H/$SO_3^-Na^+$ of PVSA unit). Whereas, Ag^+ ions and Ag NPs loaded hydrogels exhibited similar peaks with slight change in their vibrational frequencies. However, additional peaks are observed in curcumin loaded composite at 1505 cm^{-1} and 1265 cm^{-1} due to characteristic curcumin peaks.

Thermal properties of hydrogel-Ag NPs-curcumin composite

Thermal properties of composites not only provide their physical characteristics but also give information about the various components present in the composites (Fig. 8).

DSC of hydrogel, Ag^+ ions loaded hydrogel and Ag NPs loaded hydrogels have shown 76.5, 75.2, and 98.4°C (glass transition temperature) and 265.4, 253.6, and 301.2°C (onset decomposition or melting temperature) respectively, [Fig. 8(A)]. TGA analysis of the samples has exhibited weight loss at 700°C (82.5, 65.4, and 63.2% respectively) [Fig. 8(C)]. The above studies indicated that AgNPS-loaded hydrogels have, improved glass transition, melting temperatures, and more residues at 700°C due to higher thermal stabilities of silver nanoparticles. Curcumin-loaded hydrogel, curcumin-Ag^+ ions loaded hydrogel and curcumin-Ag NPs loaded hydrogel have also exhibited similar trends in both DSC and TGA studies. However, because of the presence of curcumin, the curcumin-loaded hydrogels have shown an additional peak between 175 and 201°C due to melting temperature of curcumin [Fig. 8(B)]. In addition, more weight loss is also found due to the presence of curcumin; in curcumin loaded the hydrogels [Fig. 8(D)].

Curcumin loading and release studies

The loading efficiency of curcumin into the hydrogels has been examined (Table III). It is found understood that the loading efficiency is higher in the case of Ag NPs loaded hydrogels compared with other type of hydrogels. The order of loading capacity of curcumin into the hydrogels as found is as follows Ag NPs loaded hydrogels > hydrogel > Ag^+ ions loaded hydrogels. The less loading in Ag^+ ions loaded hydrogels is due to all the PVSA sodium salt chains are bounded by Ag ions and thereby inhibiting the anchoring capacity of drug into the hydrogels.

In vitro curcumin release from the hydrogels is carried out in pH 7.4 buffer solution at 37°C. The percentage cumulative release of curcumin from the hydrogel was calculated using the equation,[35] $R = M_t/M_o \times 100$, where M_t is the amount of drug released at time t, M_o is the initial loaded drug

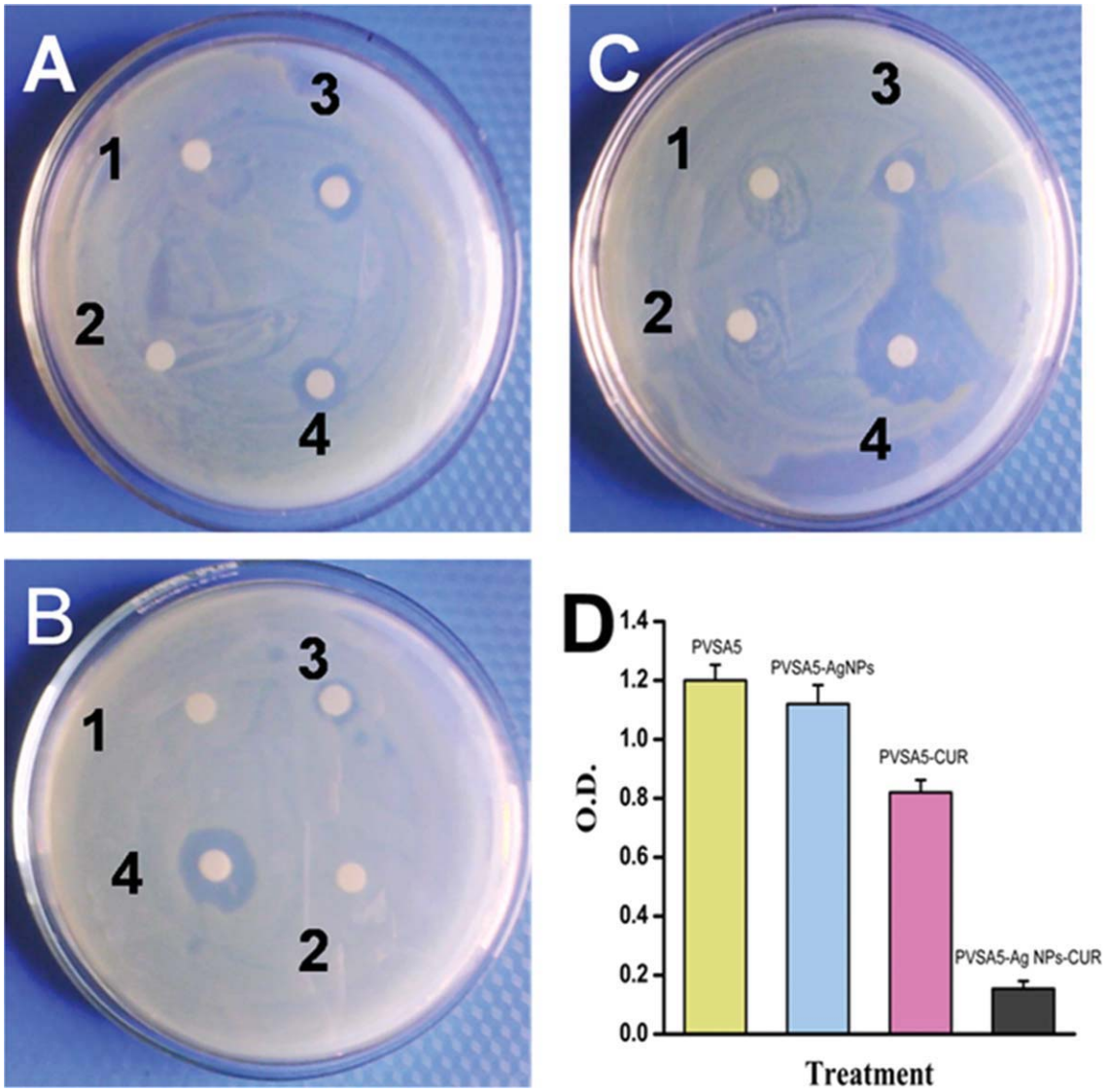

Figure 10 (A–C) Antibacterial activity of (A) PVSA2, (B) PVSA4 and (C) PVSA5 based composites against *E-coli*.[1–4] Hydrogel, hydrogel-Ag^+, hydrogel-Ag NPs and hydrogel-Ag NPs-curcumin composite. (D) Semiquantitative inhibition effects of PVSA5, hydrogel-Ag^+, hydrogel-Ag NPs and hydrogel-Ag NPs-curcumin composite against *E-coli*. [Color figure can be viewed in the online issue, which is available at wileyonlinelibrary.com.]

amount. The release profiles indicates that curcumin releases slowly from Ag NPs loaded hydrogels than hydrogels and Ag^+ ions loaded hydrogels (Fig. 9). The curcumin release data was analyzed by an equation with an empirical relationship[36] i.e., $W_t/W_\infty = kt^n$ where, W_t and W_∞ represents the amount of curcumin released at time t and at equilibrium time respectively, k is a kinetic constant related to the curcumin-polymer interaction, and n is the release exponent. The value of "n" determines the nature of the release mechanism, i.e., when $n = 0.5$ the release is Fickian diffusion mechanism and when n lies between 0.5 and 1, the release mechanism is anomalous in nature or Case II in nature. In addition if n being equal to 1, the mechanism is coined as Super Case II, the most desirable condition in controlled release technology. The release rate characteristics of curcumin from the hydrogels are presented in Table III. The lower k values for all the systems indicate a lesser interaction between the hydrogel materials and the curcumin.

Antimicrobial application

The main aim of this study is to develop a new antimicrobial/wound dressing agent. Keeping this view, new hydrogel composites are developed as antibacterial material against *E-coli*. Figure 10(A–C), illustrates the antibacterial effect of[1] pure hydrogel[2] Ag^+ ions loaded hydrogel,[3] Ag NPs loaded hydrogel and[4] hydrogel-Ag NPs-curcumin composite. The results indicates that hydrogel-Ag NPs-curcumin composites have exhibited greater reduction of *E-coli*

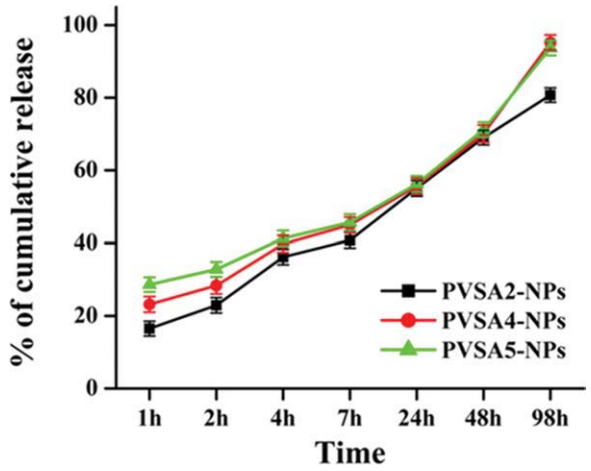

Figure 11 Silver nanoparticles release from PVSA2-Ag NPs, PVSA4-Ag NPs and PVSA5-Ag NPs hydrogels. [Color figure can be viewed in the online issue, which is available at wileyonlinelibrary.com.]

growth compared with Ag NPs loaded hydrogels. That too PVSA5 based composite has shown enormous decrease in the growth of *E-coli* than PVSA2 and PVSA4 composites. The growth rate or killing kinetics of the *E-coli* has been performed in mineral salt medium (MSM) and the results are determined by culture turbidity (O.D) measurements. Because of the presence of more number of silver nanoparticles and curcumin, PVSA5-Ag NPs-curcumin composite showed 90% inhibition growth while other hydrogel composites showed only 25% inhibition growth of *E-coli* [Fig. 10(D)]. The reason for this is two fold are the curcumin suppresses the growth of bacteria and second the release of silver nanoparticles from the hydrogel networks (PVSA5) is higher compared to other hydrogel networks (PVSA2 and PVSA4) (Fig. 11). The released silver nanoparticles from hydrogel networks can interact with sulfur containing intracellular proteins in bacteria and kill them.[8]

CONCLUSION

We have designed and developed novel hydrogel-AgNPs-curcumin composites are prepared by a simple three step approach and characterized by swelling properties, spectral, thermal, X-ray diffraction, and electronic microscopic studies. Scanning electron and Transmission electron microscopic data revealed the presence of silver nanoparticles within their networks. Furthermore, the current work demonstrates that by combining hydrogel, nanotechnology and a natural compound (curcumin) promises for developing novel antimicrobial agents with potential applications in wound dressing or burn wounds. The entrapped silver nanoparticles and curcumin molecules showed sustained release which advice enormous prolonged therapeutic values.

References

1. Ma, D.; Zhang, L.-M. J Phys Chem B 2008, 112, 6315.
2. Morones, J. R.; Frey, W. Langmuir 2007, 23, 8180.
3. Lu, Y.; Spyra, P.; Mei, Y.; Ballauff, M.; Pich, A. Macromol Chem Phys 2007, 208, 254.
4. Biffis, A.; Orlandi, N.; Corain, B. Adv Mater 2003, 15, 1551.
5. Saravanan, P.; Raju, M. P.; Alam, S. Mater Chem Phys 2007, 103, 278.
6. Wang, C.; Flynn, N. T. R Langer Adv Mater 2004, 16, 1074.
7. Wang, C.; Flynn, N. T. R. Langer Mater Res Soc Symp Proc 2004, 820, R2.2.1.
8. Murali Mohan, Y.; Lee, K.; Premkumar, T.; Geckeler, K. E. Polymer 2007, 48, 158.
9. Vimala, K.; Samba Sivudu, K.; Murali Mohan, Y.; Sreedhar, B.; Mohana Raju, K. Carbohyd Polym 2009, 75, 463.
10. Murthy, P. S. K.; Murali Mohan, Y.; Varaprasad, K.; Sreedhar, B.; Mohana Raju, K. J Colloid Interf Sci 2008, 318, 217.
11. Varaprasad, K.; Murali Mohan, Y.; Ravindra, S.; Narayana Reddy, N.; Vimala, K.; Monika, K.; Sreedhar, B.; Mohana Raju, K. J Appl Polym Sci 2010, 115, 1119.
12. Yu, H.; Xu, X.; Chen, X.; Lu, T.; Zhang, P.; Jing, X. J Appl Polym Sci 2007, 103, 125.
13. Murali Mohan, Y.; Vimala, K.; Thomas, V.; Varaprasad, K.; Sreedhar, B.; Bajpai, S. K.; Mohana Raju, K. J Colloid Interf Sci 2010, 342, 73.
14. Tian, J.; Wong, K. K. Y.; Ho, C.-M.; Lok, C.-N.; Yu, W.-Y.; Che, C.-M.; Chiu, J.-F.; Tam, P. K. H. Chem Med Chem 2007, 2, 129.
15. Atiyeh, B.; Costagliola, M.; Hayek, S.; Dibo, S. Burns 2007, 33, 139.
16. Mishra, M.; Kumar, H.; Tripathi, K. Digest J Nanomater Biostruct 2008, 3, 49.
17. Elechiguerra, J. L.; Burt, J. L.; Morones, J. R.; Camacho-Bragado, A.; Gao, X.; Lara, H. H.; Yacaman, M. J. J Nanobiotech 2005, 3, 6.
18. Maheshwari, R. K.; Singh, A. K.; Gaddipati, J.; Srimal, R. C. Life Sci 2006, 78, 2081.
19. Kim, H., II; Park, S. J.; Kim, S. J. Smart Mater Struct 2006, 15, 1882.
20. Lee, J. H.; Oh, S. H. J Biomed Mater Res 2002, 60, 44.
21. Lu, Y.; Mei, Y.; Drechsler, M.; Ballauff, M. Angew Chemie Inter Ed 2006, 45, 813.
22. Kim, S. J; Park, S. J.; Kim, S. I. Smart Mater Struct 2004, 13, 317.
23. Kim, H. I.; Park, S. J.; Kim, S. I.; Kim, N. G.; Kima, S. J. Synt Metals 2005, 155, 674.
24. Suwantong, O.; Opanasopit, P.; Ruktanonchai, U.; Supaphol, P. Polymer 2007, 48, 7546.
25. Lin, S. Y.; Chem, K. S.; Run-Chu, L. Biomater 2001, 22, 2999.
26. Purna, S. K.; Babu, M. Burns 2000, 26, 54.
27. Choates, C. S. J Am Pediatr Med Assoc 1994, 84, 463.
28. Lee, H. J.; Yeo, S. Y.; Jeong S. H. J Mater Sci 2003, 38, 2199.
29. Son, W. K.; Youk, J. H.; Lee, T. S.; Park, W. H. Macromol Rapid Commun 2004, 25, 1632.
30. Balakrishnan, B.; Mohanty, M.; Umashankar, P. R.; Jayakrishnan, A. Biomater 2005, 26, 6335.
31. Yu, S. H.; Mi, F. L.; Wu, Y. B.; Peng, C. K.; Shyu, S. S.; Huang, R. N. J Appl Polym Sci 2005, 98, 538.
32. Murali Mohan, Y.; Geckeler, K. E. React Funct Polym 2007, 67, 1445.
33. Hussain, S.; Roy, R. K.; Pal, A. K. Mater Chem Phys 2006, 99, 375.
34. Mock, J. J.; Barbic, M.; Smith, D. R.; Schultz, D. A.; Schultz, S. J. Chem Phys 2005, 116, 6755.
35. Ekici, S.; Saraydin, D. Polym Int 2007, 56, 1371.
36. Ritger, P. L.; Peppas, N. A. J Control Release 1987, 5, 37.